

Estimating matter-induced *CPT* violation in long-baseline neutrino experiments

Monika Randhawa*

University Institute of Engineering and Technology, Panjab University, Chandigarh 160014, India

Mandip Singh and Manmohan Gupta

Department of Physics, Centre of Advanced Study, Panjab University, Chandigarh 160014, India

(Received 13 February 2014; published 6 January 2015)

We examine matter-induced *CPT* violation effects in long-baseline electron neutrino appearance experiments in a low energy neutrino factory setup. Assuming *CPT* invariance in vacuum, the magnitude of *CPT* violating asymmetry in matter has been estimated using the exact expressions for the transition probabilities. The dependence of the asymmetry on the oscillation parameters like mixing angles, mass squared differences, as well as on the Dirac *CP* violating phase has been investigated.

DOI: 10.1103/PhysRevD.91.017301

PACS numbers: 14.60.Pq, 11.30.Er

I. INTRODUCTION

In particle theory, the discrete symmetries C, P, and T have a central importance. Although C, P, CP, and T are violated [1], *CPT* is a good symmetry [2] in the standard model (SM); therefore, the fundamental *CPT* violation may be connected to physics beyond the SM, such as string theory [3,4]. Experimentally, *CPT* nonconservation can be probed in the neutrino oscillations, where it would manifest itself by showing different oscillation probabilities for the transitions $\nu_\alpha \rightarrow \nu_\beta$ and $\bar{\nu}_\beta \rightarrow \bar{\nu}_\alpha$ [5,6]. In this context, although a 2010 observation of MINOS [7] reported tension between ν_μ and $\bar{\nu}_\mu$ oscillation parameters, suggesting *CPT* violation, the difference was not observed in their revised results in 2012 [8]. Nevertheless, the interest in the search of *CPT* violation continues [9], particularly owing to the increasing precision with which the oscillation parameters are being measured in the current generation of long-baseline (LBL) experiments [10–13].

Even if it is assumed that the *CPT* invariance theorem holds good, when neutrinos propagate in a material medium, the matter effects, arising due to interaction of neutrinos with an asymmetric matter, lead to *CPT* violation in neutrino oscillations, known as extrinsic or fake *CPT* violation [14,15]. The matter effects become all the more important in the long-baseline neutrino oscillation experiments, where neutrinos travel a long distance in the Earth's matter [10–13]. These fake effects should be accounted for, while searching for *CPT* violation.

The matter induced *CPT* violation has been estimated in some of the papers in the atmospheric as well as long-baseline experiments, primarily by using the approximate analytic expressions for the probabilities for various neutrino oscillation channels [15]. The validity of the various approximations depends on the baseline length and the energy of the neutrino, as well as on the mixing angle θ_{13} .

Therefore, keeping in mind the recently determined large value of θ_{13} [16], to which the appearance probabilities are very sensitive, as well as the increased precision in the measurement of other oscillation parameters, it becomes imperative to calculate the probabilities in an exact manner and to update the estimates of *CPT* asymmetry in neutrino oscillation experiments. This becomes particularly important in view of the large L and E range available to the neutrino in the ongoing and future experiments. In this regard, the channel that has been most extensively used to estimate the magnitude of *CPT* violating parameters is the disappearance channel $\nu_\mu \rightarrow \nu_\mu$ [14,15] as it offers high event rates and little beam contamination. Furthermore, the neutrino oscillation effects in this channel are large; however, it has been pointed out that the matter effects are rather small in $\nu_\mu \rightarrow \nu_\mu$ oscillations [14]. Therefore, to study the effects of matter potential, leading to extrinsic *CPT* violation, the subdominant channel $\nu_\mu \rightarrow \nu_e$ looks to be more promising. Further, this channel is the principal appearance channel available to conventional beams and superbeams. However, the corresponding *CPT* conjugate channel $\bar{\nu}_e \rightarrow \bar{\nu}_\mu$ is not going to be explored in the ongoing and forthcoming experiments [10–13], as these explore channels that are *CP* conjugate of each other. In this regard neutrino factories, which are under active consideration [17], offer a combination of *CP* and *CPT* conjugate channels, as both electron as well as muon neutrinos are present in the beam. The challenging task in a neutrino factory is to measure the sign of the charge of the produced lepton. The sign of a muon charge can be determined using a magnetized iron neutrino detector [18]. The possibility to measure the electron (or positron) charge with a magnetized liquid argon detector has also been explored [19]. Neutrino factories with their high luminosities and low backgrounds allow us to investigate the phenomenon of neutrino oscillations with unprecedented accuracy.

*monika@pu.ac.in

Assuming CPT invariance in vacuum, the purpose of this paper is to investigate the matter-induced CPT violation effects in the $\nu_\mu \rightarrow \nu_e$ transitions in four different scenarios of long-baseline neutrino oscillation experiments, e.g., S1: $L = 300$ Km and $E = 1$ GeV, S2: $L = 1300$ Km and $E = 3.5$ GeV, S3: $L = 2300$ Km and $E = 5$ GeV, S4: $L = 3000$ Km and $E = 7$ GeV, where L is the baseline length and E is the average neutrino energy. The choice of baseline and neutrino energy for the above-mentioned scenarios is motivated by experiments like T2K [10], LBNE [12], LBNO [13], etc. The energy is chosen to be below 10 GeV, as it has been suggested that for the large value of θ_{13} , a low energy neutrino factory (LENF) is better optimized [20]. The extent of extrinsic CPT violation in the $\nu_\mu \rightarrow \nu_e$ transitions has been studied by calculating the CPT asymmetry using the exact neutrino oscillation probability formulas derived using Cayley-Hamilton formalism [21]. A comparison with the approximate calculations has also been discussed. Further, the dependence of CPT violating asymmetry on the oscillation parameters like mixing angles, mass squared differences, as well as on the Dirac CP violating phase has been examined.

II. CPT VIOLATING ASYMMETRY

For the flavor transition $\alpha \rightarrow \beta$ ($\alpha, \beta = e, \mu, \tau$), the CPT violation implies that

$$P_{\alpha\beta} \neq P_{\bar{\beta}\bar{\alpha}}, \quad (1)$$

where $P_{\alpha\beta}$ ($P_{\bar{\beta}\bar{\alpha}}$) is the probability for the neutrino (anti-neutrino) flavor transition $\nu_\alpha \rightarrow \nu_\beta$ ($\bar{\nu}_\beta \rightarrow \bar{\nu}_\alpha$). In the present work, we look for the extrinsic CPT effects in the subdominant channel $\nu_\mu \rightarrow \nu_e$. The exact expression for the probability $P_{\alpha\beta}$ is quite lengthy and complicated [21,22]; therefore, in the literature, several approximate analytic expressions have been derived [23,24], wherein the probabilities have been expanded up to first or second order in small parameters like α ($\equiv \frac{\Delta m_{12}^2}{\Delta m_{23}^2}$ the hierarchy parameter) and/or the reactor mixing angle θ_{13} . In view of the large value of θ_{13} , expanding the probability only up to first order in θ_{13} takes the results away from the exact numerical values, particularly in the L/E region relevant for the LBL experiments. Therefore, it is recommended that the probabilities be expanded up to second order in both α as well as $\sin\theta_{13}$ ($\equiv s_{13}$). For example, the approximate analytic expression for the probability $P_{\mu e}$ for flavor transitions $\nu_\mu \rightarrow \nu_e$ is given as [23]

$$P_{\mu e} = \alpha^2 \sin^2 2\theta_{12} c_{23}^2 \frac{\sin^2 A \Delta}{A^2} + 4s_{13}^2 s_{23}^2 \frac{\sin^2(A-1)\Delta}{(A-1)^2} + 2\alpha s_{13} \sin 2\theta_{12} \sin 2\theta_{23} \cos(\Delta + \delta_{CP}) \times \frac{\sin A \Delta \sin(A-1)\Delta}{A(A-1)}. \quad (2)$$

Similarly, the probability $P_{\bar{e}\bar{\mu}}$ for the CPT conjugate flavor transition ($\bar{\nu}_e \rightarrow \bar{\nu}_\mu$) is given as

$$P_{\bar{e}\bar{\mu}} = \alpha^2 \sin^2 2\theta_{12} c_{23}^2 \frac{\sin^2 A \Delta}{A^2} + 4s_{13}^2 s_{23}^2 \frac{\sin^2(A+1)\Delta}{(A+1)^2} + 2\alpha s_{13} \sin 2\theta_{12} \sin 2\theta_{23} \cos(\Delta + \delta_{CP}) \times \frac{\sin A \Delta \sin(A+1)\Delta}{A(A+1)}. \quad (3)$$

In the above expressions (2)–(3), $s_{ij} = \sin\theta_{ij}$, $c_{ij} = \cos\theta_{ij}$ ($ij \equiv 12, 23, 13$), δ_{CP} is the leptonic Dirac CP violation phase, and

$$A = \frac{2EV}{\Delta m_{31}^2}, \quad \Delta = \frac{\Delta m_{31}^2 L}{4E}, \quad (4)$$

where V is the matter potential, which gives the charged current contribution of electron neutrinos to the matter potential, L is the baseline length, E is the neutrino energy, and Δm_{31}^2 gives the atmospheric mass squared difference. The CPT invariance implies that, in vacuum, the probabilities $P_{\mu e}$ and $P_{\bar{e}\bar{\mu}}$ are exactly the same, resulting in their difference being zero, i.e.,

$$P_{\mu e} - P_{\bar{e}\bar{\mu}} = 0. \quad (\text{in vacuum, where } A = 0). \quad (5)$$

However, in matter, as mentioned earlier, the oscillation probabilities are modified due to interaction of electron neutrinos with matter particles, leading to the fake CPT violation, measured in terms of the CPT asymmetry, given for $\nu_\mu \rightarrow \nu_e$ transition as

$$A_{\mu e}^{CPT} = \frac{P_{\mu e} - P_{\bar{e}\bar{\mu}}}{P_{\mu e} + P_{\bar{e}\bar{\mu}}}. \quad (6)$$

Defining the asymmetry as the ratio of probabilities has the advantage that, on the level of event rates, the systematic experimental uncertainties cancel out to a large extent.

III. INPUTS

Before going into the details of the analysis, we mention some of the essentials pertaining to various inputs. The inputs for neutrino masses, mixing angles, and the leptonic Dirac CP violation phase used in the present analysis at 1 σ C.L. are as below [25]:

$$\Delta m_{12}^2 = 7.54_{-0.22}^{+0.26} \times 10^{-5} \text{ eV}^2, \quad \Delta m_{23}^2 = 2.43_{-0.10}^{+0.06} \times 10^{-3} \text{ eV}^2, \quad (7)$$

$$\sin^2 \theta_{12} = 0.307_{-0.016}^{+0.018}, \quad \sin^2 \theta_{23} = 0.386_{-0.021}^{+0.024}, \quad (8)$$

$$\sin^2\theta_{13} = 0.0241 \pm 0.0025, \quad \delta_{CP} = 1.08_{-0.31}^{+0.28}\pi. \quad (9)$$

In the present work, we consider the baseline length $L \leq 3000$ Km, implying that one can assume the neutrinos to be traveling in the constant matter density of the Earth's crust. The matter potential V varies with the density ρ of the matter, and for the Earth's crust's density ($\rho_{\text{crust}} \approx 3\text{g/cm}^3$) is given as $V \approx 11.34 \times 10^{-14}$ eV.

IV. NUMERICAL ANALYSIS AND RESULTS

Using the exact neutrino oscillation probability formulas derived using Cayley-Hamilton formalism [21] and the input parameters given in Eqs. (7)–(9) at their best fit values, we have numerically calculated the CPT asymmetry for various scenarios of L and E , as presented in Table I. The values of $A_{\mu e}^{CPT}$ calculated using the approximate expressions of the probabilities have also been presented in the table.

We observe from Table I that the magnitude of the CPT asymmetry in these experiments is not small; particularly for baselines greater than 1000 Km, the asymmetry is large enough. However, it should be kept in mind that due to the oscillatory behavior of the CPT asymmetry, the magnitude of the asymmetry may vary greatly on the slightest variation of the neutrino energy E and/or the baseline length L . Therefore, it is more appropriate to graphically show the variation of $A_{\mu e}^{CPT}$ with neutrino energy E .

In Fig. 1, we have plotted the approximate as well as the exact magnitude of $A_{\mu e}^{CPT}$ as a function of neutrino energy E for the four baselines given in Table I. The upper limit of the energy range chosen corresponds to the range available to the LENS. All other input parameters have been kept at their best fit values given in Eqs. (7)–(9). It may be mentioned that the neutrinos have been assumed to follow normal hierarchy of masses throughout this work. We observe that the peak value of the CPT asymmetry $A_{\mu e}^{CPT}$ increases with increasing neutrino energy. This behavior is expected, as the matter effects increase with the neutrino energy. Further, for a given energy, $A_{\mu e}^{CPT}$ is maximum for S4 and minimum for S1, implying that $A_{\mu e}^{CPT}$ increases with baseline length. On comparing the four plots in Fig. 1, we find that the rise in $A_{\mu e}^{CPT}$ per unit increase in energy is maximum for S4, implying that the longer the baseline, the

more sensitivity of $A_{\mu e}^{CPT}$ towards the neutrino energy. Thus, it may be inferred that extrinsic CPT violation may have a significant magnitude for long-baseline neutrino oscillation experiments.

As far as the validity of the approximate analytical expressions is concerned, the plots reveal that the agreement between the approximate and the exact calculations is better at higher energies in comparison to lower energies. This is due to the reason that the approximate expressions for the probabilities given in Eqs. (2)–(3) are valid only when $L/E \ll 10^4$ Km/GeV, i.e., far from the L/E region where the low frequency solar oscillations become dominant. Therefore, one must be careful about the region, where the approximate analytic formulas may be applied.

In Fig. 2, we present the exact calculations of $A_{\mu e}^{CPT}$ as functions of E and L . The dots indicate the baseline length L and the average neutrino energy E for various experimental scenarios given in Table I. An assumed energy spread of 20% in the beam is indicated by the error bars. It is clear from the figure that $A_{\mu e}^{CPT}$ is maximum at the upper right corner, where both E and L are large. At the lower right corner $A_{\mu e}^{CPT}$ is too small to be of significance. The effect of extrinsic CPT violation is maximum for S3 and S4, where it is between 0.6 and 0.8. For S1 and S2 it is less than 0.4. Further, it may be seen that $A_{\mu e}^{CPT}$ values will not change significantly within the whole spread of energy for S1 and S2; however, for S3 and S4, $A_{\mu e}^{CPT}$ may become larger at the lower end of the energy dispersion. Thus, for these experiments the effect of extrinsic CPT violation is not only large, but will further increase at neutrino energies that are lower than the average value. However, these results should be interpreted rather carefully, since in real experiments the detectors have a finite energy resolution; very fast oscillations at low energies cannot be resolved. Therefore, one should consider probabilities averaged over the energy resolutions of the detectors. Moreover, to make any final comment about the magnitude of the CPT asymmetry in any experiment, it is of utmost importance to mention that the two CPT conjugate channels should be compared in terms of neutrino event rates, which, apart from the oscillation probabilities, also depend on neutrino-nucleon cross section and initial flux of neutrinos. In the present work, however, we confine our analysis to the study of oscillation probabilities only. The analysis with event rates will be discussed in a future publication.

It is interesting to note that $A_{\mu e}^{CPT}$ is very sensitive to variations in θ_{23} , θ_{13} , and Δm_{23}^2 , while variations in θ_{12} , Δm_{12}^2 , and δ_{CP} hardly affect $A_{\mu e}^{CPT}$. Our analysis shows that the sensitivity of $A_{\mu e}^{CPT}$ towards θ_{23} , θ_{13} , and Δm_{23}^2 increases with increasing baseline length and decreases with increasing values of the average neutrino energy. However, at longer baseline lengths the effect of L is more pronounced than the effect of energy. Therefore, despite having a high value of average energy E , the S4 setup has the highest

TABLE I. CPT asymmetry $A_{\mu e}^{CPT}$ for various scenarios of L and E . All other input parameters are kept at their best fit values given in Eqs. (7)–(9).

Scenario	L (Km)	E (GeV)	$A_{\mu e}^{CPT}$ exact	$A_{\mu e}^{CPT}$ approximate
S1	300	1.0	0.058	0.058
S2	1300	3.5	0.31	0.30
S3	2300	5.0	0.63	0.62
S4	3000	7.0	0.73	0.72

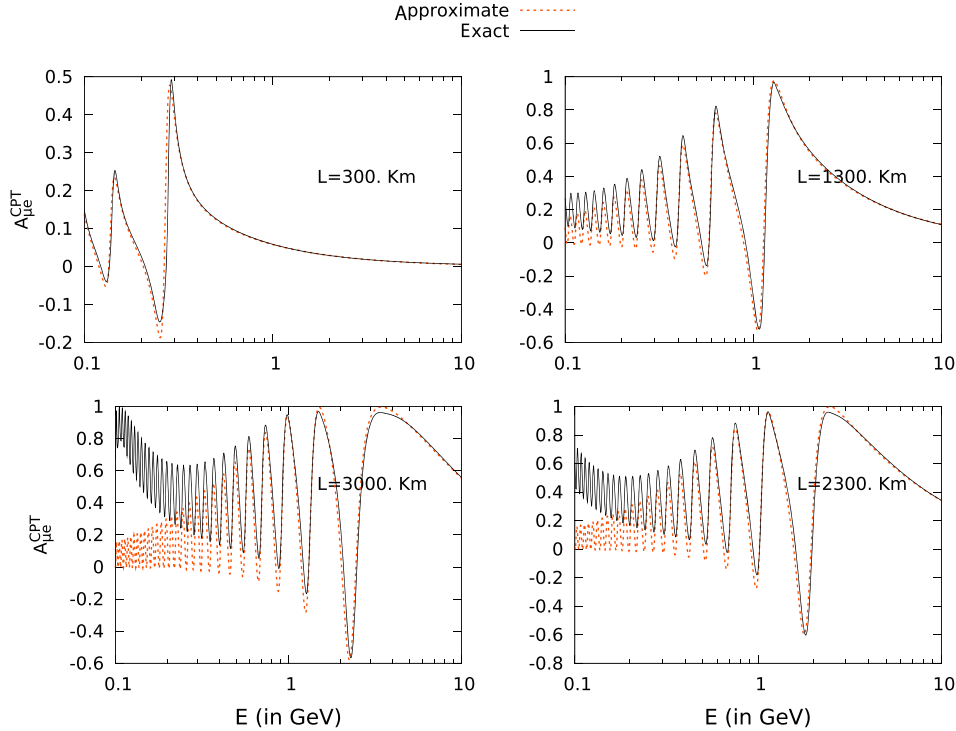


FIG. 1 (color online). CPT asymmetry $A_{\mu e}^{CPT}$ plotted as a function of neutrino energy E , for the baseline lengths corresponding to four scenarios given in Table I. The dotted curves correspond to approximate calculations using Eq. (6), whereas the solid curves correspond to the exact numerical calculations. All other input parameters are kept at their best fit values given in Eqs. (7)–(9).

sensitivity towards variation in θ_{23} , θ_{13} , and Δm_{23}^2 followed by S3, S2, and S1, in that order. For example, for S4, at the upper limit of θ_{13} , $A_{\mu e}^{CPT}$ increases from 0.3 to 0.6, all other parameters being at their mean values. These results assume significance in the wake of the fact that the precision in the determination of $\sin^2\theta_{13}$ is less in comparison to other parameters. Further, it is worth noting that though $A_{\mu e}^{CPT}$

values change very little with δ_{CP} in the L/E region relevant for various experimental scenarios discussed in the text, in the low E and longer L region, $A_{\mu e}^{CPT}$ varies significantly with δ_{CP} as shown by the thick black curve in Fig. 3, which corresponds to $L = 3000$ Km and $E = 0.5$ GeV. All other lines in the figure, corresponding to the experimental scenarios given in Table I, are almost insensitive to variations in δ_{CP} . This is due to the reason that the probability itself is large in the low E region, and hence also is more sensitive to the variation of δ_{CP} . Thus, it may be said that the magnitude

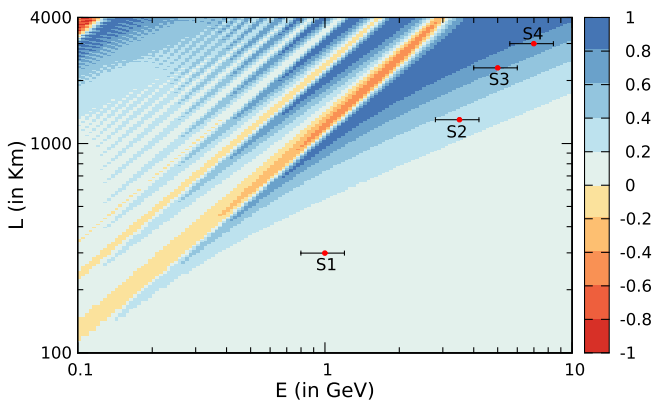


FIG. 2 (color online). CPT asymmetry $A_{\mu e}^{CPT}$ as a function of neutrino energy E and baseline length L . The dots correspond to L and average energy E of the experimental scenarios given in Table I, while an assumed energy spread of 20% in the beam is indicated by the error bars. All other input parameters are kept at their best fit values given in Eqs. (7)–(9).

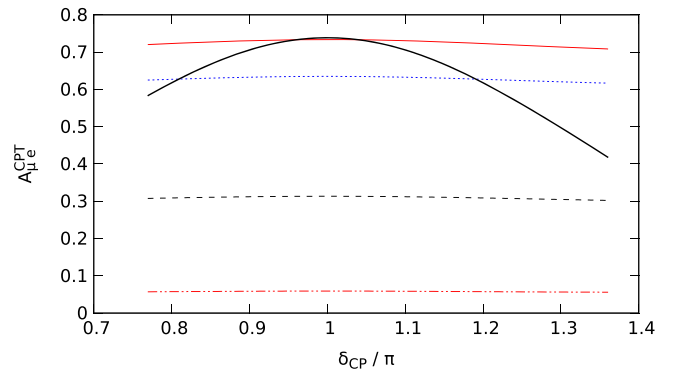


FIG. 3 (color online). CPT asymmetry $A_{\mu e}^{CPT}$ as a function of CP violation phase δ_{CP} for the scenarios S1, S2, S3, and S4. The thick black curve corresponds to $L = 3000$ Km and $E = 0.5$ GeV.

of CPT asymmetry is sensitive to the magnitude of CP violation in the high L/E region.

V. CONCLUSIONS

In conclusion, we have investigated the implications of matter-induced CPT violation effects on the transition probabilities for neutrino oscillations in some scenarios of long-baseline electron neutrino appearance experiments, in a low energy neutrino factorylike setup. We find that the magnitude of CPT asymmetry $A_{\mu e}^{CPT}$ in these experiments is not ignorable; particularly for baselines greater than 1000 Km, the asymmetry is large enough. The peak value of the CPT asymmetry increases with increasing neutrino energy as well as with baseline length. We have also examined the dependence of CPT violating asymmetry on the oscillation parameters like mixing angles, mass squared differences, as well as on the Dirac CP violating phase for

these long-baseline experiments. We observe that $A_{\mu e}^{CPT}$ is very sensitive to variation in θ_{23}, θ_{13} , and Δm_{23}^2 , while the variations in $\theta_{12}, \Delta m_{12}^2$ hardly affect $A_{\mu e}^{CPT}$. Although $A_{\mu e}^{CPT}$ values change very little with δ_{CP} , we observe that in the low E and longer L region, $A_{\mu e}^{CPT}$ varies significantly with δ_{CP} , suggesting that the magnitude of CPT asymmetry is sensitive to the magnitude of CP violation in the high L/E region. It is suggested that the experimental collaborations should investigate the effects of extrinsic CPT violation in their respective experimental setups.

ACKNOWLEDGEMENTS

M. S. thanks the Chairman, Department of Physics for providing facilities to work. M. R. is supported by the University Grants Commission, Government of India, under the Research Award Scheme [Grant No. F.30-39/2011(SA-II)].

-
- [1] I. I. Bigi and A. I. Sanda, *CP Violation* (Cambridge University Press, Cambridge, 2009) and references therein.
- [2] S. Weinberg, *The Quantum Theory of Fields* (Cambridge University Press, Cambridge, 2005) and references therein.
- [3] V. A. Kostelecky and R. Potting, *Nucl. Phys.* **B359**, 545 (1991); *Phys. Rev. D* **51**, 3923 (1995).
- [4] D. Colladay and V. A. Kostelecky, *Phys. Rev. D* **55**, 6760 (1997); **58**, 116002 (1998).
- [5] N. Cabibbo, *Phys. Lett.* **72B**, 333 (1978); V. Barger, K. Whisnant, and R. J. N. Phillips, *Phys. Rev. Lett.* **45**, 2084 (1980); S. Pakvasa, in *Proc. of the XXth International Conference on High Energy Physics*, edited by L. Durand and L. G. Pondrom, AIP Conf. Proc. No. 68 (AIP, New York, 1981), Vol. 2, p. 1164.
- [6] O. W. Greenberg, *Phys. Rev. Lett.* **89**, 231602 (2002).
- [7] P. Adamson *et al.* (MINOS), *Phys. Rev. Lett.* **107**, 021801 (2011).
- [8] P. Adamson *et al.* (MINOS), *Phys. Rev. Lett.* **108**, 191801 (2012).
- [9] V. A. Kostelecky and M. Mewes, *Phys. Rev. D* **69**, 016005 (2004); Jorge S. Diaz, V. A. Kostelecky, and M. Mewes, *Phys. Rev. D* **80**, 076007 (2009); Jorge S. Diaz and V. A. Kostelecky, *Phys. Lett. B* **700**, 25 (2011); *Phys. Rev. D* **85**, 016013 (2012).
- [10] K. Abe *et al.* (T2K Collaboration), *Nucl. Instrum. Methods Phys. Res., Sect. A* **659**, 106 (2011); K. Abe *et al.*, *Phys. Rev. Lett.* **107**, 041801 (2011).
- [11] R. Patterson (NOvA Collaboration), *Nucl. Phys. B, Proc. Suppl.* **235–236**, 151 (2013).
- [12] C. Adams *et al.* (LBNE Collaboration), arXiv:1307.7335.
- [13] A. Stahl *et al.*, Reports No. CERN-SPSC-2012-021 and No. SPSC-EOI-007.
- [14] M. C. Banuls, G. Barenboim, and J. Bernabeu, *Phys. Lett. B* **513**, 391 (2001).
- [15] Z. Z. Xing, *J. Phys. G* **28**, B7 (2002); J. Bernabeu, S. Palomares-Ruiz, A. Perez, and S. T. Petcov, *Phys. Lett. B* **531**, 90 (2002); M. Jacobson and T. Ohlsson, *Phys. Rev. D* **69**, 013003 (2004); Anindya Datta, Raj Gandhi, Poonam Mehta, and S. Uma Sankar, *Phys. Lett. B* **597**, 356 (2004); T. Ohlsson and S. Zhou, arXiv:1408.4722.
- [16] F. An *et al.* (Daya Bay Collaboration), *Phys. Rev. Lett.* **108**, 171803 (2012); J. Ahn *et al.* (RENO collaboration), *Phys. Rev. Lett.* **108**, 191802 (2012).
- [17] S. Geer, *Phys. Rev. D* **57**, 6989 (1998); **59**, 039903(E) (1999); V. D. Barger, S. Geer, R. Raja, and K. Whisnant, *Phys. Rev. D* **62**, 013004 (2000); M. Freund, M. Lindner, S. T. Petcov, and A. Romanino, *Nucl. Phys.* **B578**, 27 (2000); C. Albright *et al.*, Report No. FERMILAB-FN-692; M. Freund, P. Huber, and M. Lindner, *Nucl. Phys.* **B615**, 331 (2001).
- [18] A. Cervera, A. Laing, J. Martin-Albo, and F. Soler, *Nucl. Instrum. Methods Phys. Res., Sect. A* **624**, 601 (2010); R. J. Abrams *et al.* (IDS-NF Collaboration), arXiv:1112.2853; A. Bross *et al.*, *Phys. Rev. ST Accel. Beams* **16**, 081002 (2013).
- [19] J. Tang and W. Winter, *Phys. Rev. D* **81**, 033005 (2010); E. Fernandez Martinez, T. Li, S. Pascoli, and O. Mena, *Phys. Rev. D* **81**, 073010 (2010); P. Ballett and S. Pascoli, *Phys. Rev. D* **86**, 053002 (2012).
- [20] S. Agarwalla, P. Huber, J. Tang, and W. Winter, *J. High Energy Phys.* **01** (2011) 120.
- [21] T. Ohlsson, *Phys. Scr.* **T93**, 18 (2001).
- [22] Z. Z. Xing, *Phys. Lett. B* **487**, 327 (2000); K. Kimura, A. Takamura, and H. Yokomakura, *Phys. Rev. D* **66**, 073005 (2002).
- [23] E. K. Akhmedov, R. Johansson, M. Lindner, T. Ohlsson, and T. Schwetz, *J. High Energy Phys.* **04** (2004) 078.
- [24] J. Arafune, M. Koike, and J. Sato, *Phys. Rev. D* **56**, 3093 (1997); M. Freund, *Phys. Rev. D* **64**, 053003 (2001); O. Peres and A. Y. Smirnov, *Nucl. Phys.* **B680**, 479 (2004).
- [25] G. L. Fogli, E. Lisi, A. Marrone, D. Montanino, A. Palazzo, and A. M. Rotunno, *Phys. Rev. D* **86**, 013012 (2012).